PCCP

Accepted Manuscript

ROYAL SOCIETY OF CHEMISTRY

www.rsc.org/pccp

Physical Chemistry Chemical Physics
CREATED USING THE RSC LaTeX PCCP ARTICLE TEMPLATE – SEE www.rsc.org/electronicfiles FOR DETAILS
ARTICLE TYPE www. rsc.org/xxxxxx | XXXXXXXX

Mechanisms of Hydrogen Bond Formation between Ionic Liquids and Cellulose and the Influence of Water Content†

Brooks D. Rabideau* and Ahmed E. Ismail

Received Xth XXXXXXXXXX 20XX, Accepted Xth XXXXXXXXX 20XX
First published on the web Xth XXXXXXXXXX 200X
DOI: 10.1039/b000000x

We study the dynamics of the formation of multiple hydrogen bonds between ionic liquid anions and cellulose using molecular dynamics simulations. We examine fifteen different ionic liquids composed of 1-alkyl-3-methylimidazolium cations ([$C_n$mim], $n = 1,2,3,4,5$) paired with either chloride, acetate or dimethylphosphate. We map the transitions of anions hydrogen bonded to cellulose into different bonding states. We find that increased tail length in the ionic liquids has only a very minor effect on these transitions, tending to slow the dynamics of the transitions and increasing the hydrogen bond lifetimes. Each anion can form up to four hydrogen bonds with cellulose. We find that this hydrogen bonding "redundancy" increases the binding lifetime of anions with cellulose by roughly 3 to 4 times the lifetime of a singly bound anion and account for roughly half of all hydrogen bonds between the anions and cellulose. Additional simulations for [C_2mim]Cl, [C_2mim]Ac and [C_2mim]DMP were performed at different water concentrations between 70 mol % and 90 mol %. It was found that water crowds the hydrogen bond accepting sites of the anions, preventing interactions with cellulose. The more water that is present in the system, the more crowded these sites become. Thus, if a hydrogen bond between an anion and cellulose breaks, the likelihood that it will be replaced by one of the waters in abundance increases as well. We show that the formation of these "redundant" hydrogen bonding states is greatly affected by the presence of water, leading to steep drops in hydrogen bonding between the anions and cellulose.

1 Introduction

Exploiting lignocellulosic biomass as a replacement feedstock for manufacturing processes that currently rely on petroleum and other fossil-fuel based feedstocks is a critical goal for environmentally sustainable manufacturing. While a number of laboratory-scale processes for treating biomass have already been developed, the recalcitrance of lignocellulosic biomass to traditional dissolution processes has hindered the development of industrial-scale processes for biomass conversion. Native plant cellulose, composed primarily of cellulose Iβ,[1] displays a hierarchy of dense intra- and intermolecular forces that hold the individual strands of cellulose together as a crystalline bundle. Hydrogen bonds between neighboring glucan units impart rigidity to the individual strands,[2] while hydrogen bonds between neighboring strands facilitate the formation of cellulose sheets.[3] These sheets are in turn held tightly together by strong hydrophobic forces.[4] Additionally, the morphology and faceting of the cellulose bundles can further affect these interaction strengths.[5–7] Together, the dense hydrophobic and hydrophilic interactions make cellulose very resistant to breakup and relatively few solvent media have proven capable of successfully breaking down cellulose.

Among the solvents that have been demonstrated to work are ionic liquids (ILs), and in particular the class of 1-alkyl-3-methylimidazolium cations, paired with anions such as chloride, acetate, or dimethylphosphate.[8] ILs have been shown to expand and distort the crystalline lattice prior to dissolution[9] and can initiate conformational changes in cellulose's structure.[10–12] Upon regeneration in water, formation of cellulose II is observed.[13] Interestingly, water is unable to dissolve cellulose and even in minor amounts its presence can affect the properties of an IL,[14,15] precluding dissolution.[16,17] Furthermore it has been shown that the presence of co-solvents can enhance the dissolution process.[18–21] A lot of effort has been directed at finding the ideal combination of anion and cation for dissolution and the maximization of glucose yields following enzymatic hydrolysis.[22–25] It has been suggested that the anions play a large role in dissolution, breaking the dense hydrogen bond network within cellulose through the formation of new hydrogen bonds,[26,27] which is supported by results showing that high hydrogen basicity is associated with cellulose dissolution.[24,28–32]

The role of the cation, however, remains less clear. Some studies report that cations can form weak hydrogen bonds with cellulose[33–35] while others conclude that they provide substantial van der Waals interactions.[36,37] Simulations seem to

RWTH Aachen University, Aachener Verfahrenstechnik, Schinkelstrasse 2, Aachen, Germany. Fax: +49 (0)241 80 628498; Tel: +49 (0)241 80 99206; E-mail: brooks.rabideau@avt.rwth-aachen.de, aei@alum.mit.edu
† Electronic Supplementary Information (ESI) available: Transition pathways for interactions of ionic liquids with cellulose Iβ bundles. See DOI: 10.1039/b000000x/

show that the cation position is primarily dictated by the location of the anions.[38,39] Recently, molecular dynamics simulations of small bundles showed that cations can intercalate between neighboring cellulose strands and actively participate in the breakup process.[40] Due to the amphiphilic nature of cellulose it is clear that solvents must be able to satisfy both the hydrophilic and hydrophobic domains.[41]

Thus, ILs should not only be able to form new hydrogen bonds with cellulose but must also be able to disrupt the strong hydrophobic forces holding sheets together.[42,43] Simulations examining the interactions of 15 different imidazolium-based ILs recently showed that ILs at the surface of individual cellulose strands form a patchwork wherein anions interact with the hydrophilic domains while the cations interact with the hydrophobic domains.[44] Although most studies acknowledge the important role that hydrogen bonds between IL anions and cellulose play in solvation, few studies have focused on the detailed interactions and the formation and destruction mechanisms of these bonds. The ability of chloride and acetate ions to form simultaneous hydrogen bonds with separate hydroxyl units within cellulose has been noted before[37,45] and we would generally expect increased solvation for anions forming more, stronger and longer-lived hydrogen bonds. A deeper understanding of the detailed dynamics of these anions with cellulose should help in the design of newer and better solvents of cellulose.

In this paper we examine the complex mechanisms of hydrogen bond formation and destruction between the anions. We find anions can bind in a myriad of different ways with the multiple hydroxyl groups of cellulose. Interestingly there is a complex pattern of transitions from one binding state to the next, which facilitates the formation of simultaneous hydrogen bonds with a single anion. This simultaneous binding state significantly increases the binding lifetime.

2 Methods

Following our prior study of small cellulose bundles in dimethylimidazolium dimethylphosphate, 1-ethyl-3-methylimidazolium acetate, and 1-butyl-3-methylimidazolium chloride,[40] we now study a set of fifteen ionic liquids, formed by considering methyl, ethyl, propyl, butyl and pentyl tails in the 1-alkyl-3-methylimidazolium series with chloride, acetate, and dimethylphosphate anions (see fig. 1). For brevity we denote the ILs as $[C_n\text{mim}]Y$, where n is the number of carbons in the alkyl tail and Y is either chloride (Cl), acetate (Ac) or dimethylphosphate (DMP).

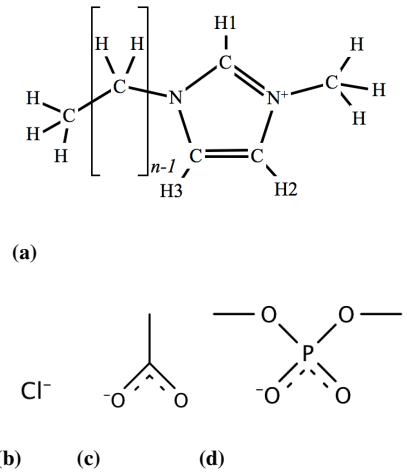

Fig. 1 Chemical structures of the ionic liquids of the present study: (a) A 1-alkyl-3-methylimidazolium cation $[C_n\text{mim}]^+$, (b) chloride $[\text{Cl}]^-$, (c) acetate $[\text{Ac}]^-$ and (d) dimethylphosphate $[\text{DMP}]^-$.

2.1 Simulation Details

All simulations were performed using LAMMPS.[46] The simulation cell contained a single strand of cellulose comprised of 16 glucose units in a previously equilibrated sample of one of the 15 different ionic liquids studied. The initial state of the cellulose strand was elongated and taken from the crystallography data of the cellulose Iβ state.[3] Prior to this each solvent was placed in a $60\,\text{Å} \times 60\,\text{Å} \times 100\,\text{Å}$ simulation cell and equilibrated in an *NPT* ensemble at 400 K and 1 bar for 3 ns using a Nosé-Hoover thermostat and barostat with coupling constants of 100 fs and 1000 fs, respectively. Next, the elongated cellulose strand was placed in the equilibrated solvent, with cations and anions removed in a 1:1 ratio to provide space for the cellulose strand. The resulting system was then simulated for another 3 ns in an *NPT* ensemble at 400 K and 1 bar and then continued in an *NVT* ensemble at 400 K for approximately 40 ns. Additional simulations were performed using small cellulose Iβ bundles (10 strands, 8 glucose units per strand) as outlined in our previous paper.[40] These simulations were performed in precisely the same manner as the simulations with the individual strands.

To study the influence of water content on the mechanisms of hydrogen bond formation, we studied aqueous mixtures of the ionic liquids $[C_2\text{mim}]$Cl, $[C_2\text{mim}]$Ac and $[C_2\text{mim}]$DMP with water contents of 70 mol%, 80 mol% and 90 mol%. In a previous study examining similar ILs, this concentration range corresponded to a major transition in the structure of the IL/water mixture from an ionic liquid with dissolved water to an aqueous solution with the IL as a dissolved component.[14] These additional simulations were also conducted using the

same methodology as the pure IL simulations outlined above.

The IL cations and chloride were modeled using the systematic force field developed by Canongia Lopes et al.[47,48] Cellulose and the remaining anions were modeled using the OPLS-2005 all-atom force field.[49] The TIP3P model was used for water.[50] The cationic C–H bonds and the bonds and angles of the water molecules were constrained using the SHAKE algorithm.[51] Electrostatic and dispersion interactions were calculated using a cutoff of 12 Å and long-range electrostatic interactions computed with the particle-particle particle-mesh algorithm[52] with an accuracy of 10^{-4}. Atomic positions were collected every 20 ps and used for the analysis.

2.2 Analysis

2.2.1 Hydrogen Bonding Hydrogen bonds occurring between the cellulose strand and the anion of each IL were computed using a set of geometric criteria.[53–58] Assuming a hydrogen bond of the form O−H···X, in which X designates either chloride, the acetate oxygens, the dimethylphosphate oxygens, or the water oxygen these criteria require an O−X distance less than 3.5 Å, an H−X distance less than 2.45 Å and an HOX angle that is less than 30°. Recently, it was shown that the set of geometric criteria one uses can significantly effect the local hydrogen bond network in neat imidazolium-based chlorides.[59,60] To ensure that our criteria do not significantly effect our results we produced histogram plots as a function of the length and angular criteria for each of the anion types. This data showed that our choice of criteria encapsulates the overwhelming majority of the regions that can be attributed to the hydrogen bonds. Furthermore, we re-analyzed our results using a much larger angular criteria of 60°, observing very few differences with our standard set of criteria. These additional results can be found in the Supporting Information.

Trajectories were collected every 20 ps, and hydrogen bonds that appeared in two successive frames were deemed to have remained intact during the intervening time period and considered a persistent hydrogen bond. Given the results that we will show later, where contacts between the IL anions and cellulose often persisted for more than 1 ns, such an assumption is reasonable. Caution, however, should be taken in interpreting values less than or equal to 20 ps. These values provide us with rough estimates for these very short lifetimes and more focus should be directed upon the relative speed of these transitions relative to the others.

2.2.2 Notation of Binding States The interactions of individual anions with multiple hydroxyl groups within cellulose can produce diverse hydrogen bond configurations, referred to here as "states". While chloride has only one site that can receive hydrogen bonds, acetate has two sites and dimethylphosphate four. Multiple hydrogen bonds are able to form with each of these sites. The overall state of an anion can be characterized by hydrogen bonds formed between separate hydroxyl groups with a single anion site (S-type), separate hydroxyl groups with separate anion sites (B-type) or a single hydroxyl group with separate anion sites (V-type). Since some states can contain multiple binding types (e.g., both B- and V-types) naming preference is given to the most complex type present with V being the most complex, B intermediate in complexity and S the last. Since a single anion can have up to four sites that can form multiple hydrogen bonds we denote these states with up to four subscripts. For example, dimethylphosphate has four binding sites, which are denoted by four subscripts and a state given by V_{klmn} would indicate a V-type state with k and l hydrogen bonds on the POO^- oxygens and m and n hydrogen bonds on the methylated oxygens. Acetate has only two binding sites and thus has up to two subscripts while chloride has only one site and is always referred to as an S-type with one subscript. Because the anions have specific sites that are indistinguishable from one another, aside from the POO^- and methylated oxygens in dimethylphosphate, the numbering within pairs of subscripts are also indistinguishable (e.g., $B_{12} = B_{21}$ and $V_{1020} = V_{0120} = V_{0102} = V_{1002}$, but $V_{1020} \neq V_{2001}$). Examples of some of these different states are illustrated in fig. 2. The simulations of the IL-water mixtures

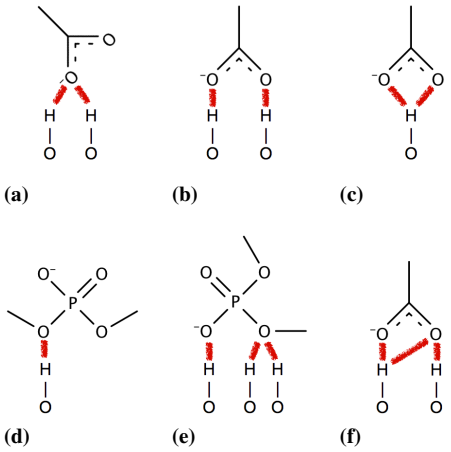

Fig. 2 (a) S_{02}, (b) B_{11}, (c) V_{11}, (d) S_{0001}, (e) B_{0102} and (f) V_{12}.

had additional bonding states compared to the pure IL systems. Some examples of these additional states are given in fig. 3. To avoid further complexity in the notation of states, we continue to use the notation outlined above, which is dictated by the bonds formed between anions and cellulose. Further information about the bonding of water to these states will simply be mentioned alongside the state (fig. 3(a)). Additionally, waters that bridge anions with cellulose (fig. 3(b)) are noted as though there is a direct anion–cellulose H-bond

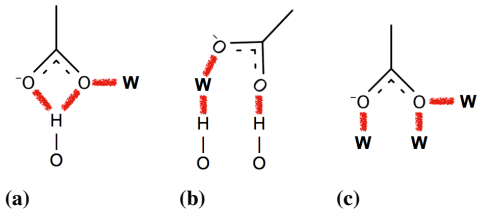

Fig. 3 Additional binding states that include water (represented as W in figure) showing (a) a V_{11} state with an individually bound water with one of the acetate oxygens, (b) a B_{11} state with a bridging water and (c) an S_{00} state with 3 individually bound waters.

and it will simply be noted that one of the bonds is a result of a water bridge. Finally, because of the additional molecular type, anions can now be bonded solely to water (fig. 3(c)). We have tracked these anions and included them in our analysis. The addition of these states now allow us to track how anions initially bind with cellulose, the effect that bound water has on the transition from state to state and should allow us to decisively determine whether or not these bridging waters help facilitate the transitions between various states.

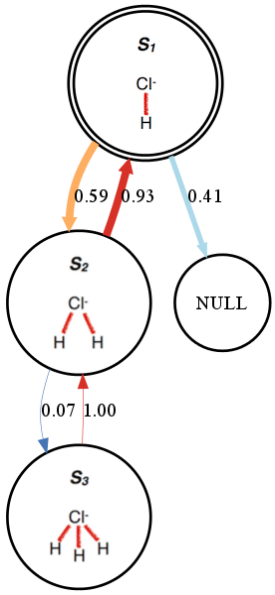

Fig. 4 H-bond transitions between different states for [C_2mim]Cl. Line width indicates the number of transitions between states. Color and arrow labels indicate the probability of the given path being taken.

3 Results and Discussion

3.1 Pure Ionic Liquids

3.1.1 Transition Pathways We first examined the transitions and populations of the different binding states that were observed during each of the simulations. The transition networks for [C_2mim]Cl, [C_2mim]Ac and [C_2mim][DMP] are given in figs. 4 to 6. In these figures, the weight of the arrows between individual states indicates the number of transitions occurring during the simulation, while the numbers next to the arrows and the colors indicate the probability of the given path being taken with red indicating transitions of high probability and blue indicating transitions of low probability. The probability of a given transition is calculated as the total number of instances of that transition normalized by the total number of instances of all transitions originating from that state. While chloride had a very linear transition pathway, moving back and forth stepwise between S_1, S_2, and S_3 (see fig. 4), acetate and dimethylphosphate had substantially more complex transition networks.

Examining [C_2mim]Ac, the hydrogen bonding first begins with the S_{01} state (indicated by double circles in figs. 4 to 6). From the S_{01} state, the acetate anion can do one of three things: it can form a second hydrogen bond with a second hydroxyl group and move to either the S_{02} state or the B_{11} state; it can form a second hydrogen bond with the same hydroxyl group moving it to the V_{11} state; or its single hydrogen bond can break and it can become an anion free of hydrogen bonds, which we denote by the NULL state. Of these different options, the longest-lasting state is the bridging state B_{11}; by contrast, the transition to the V_{11} state occurs the least frequently, and is the most unstable, as it transitions almost immediately back to the S_{01} state. The same basic pattern is observed for the other V-states observed, with nearly instantaneous transitions back to a B- or S-state. Notice that the figure shows the largest number of transitions between the S_{02} and the B_{11} states with the transition frequency favoring formation of B_{11}. The equivalent transition pathway for dimethylphosphate can be found in fig. 6. While it has greater complexity than the diagram shown for acetate, the major transitions appear to be between the analogous S_{0200} and B_{1100} states.

The transition network for the DMP anion is much more complicated than the Ac pathway, with the most frequently observed states being more interconnected with one another. For instance, S_{0100} can connect directly with every other possible state observed other than B_{1200}. Although there are more possible connections, we observe that the hydrogen bonds, as expected, are formed primarily with the nonmethylated oxygens; hydrogen bonds with the methylated oxygens are extremely unstable, and generally decompose in less than 10 ps.

3.1.2 Population of States Although figs. 4 to 6 show the presence of many diverse binding states, many of these states are rather short-lived, acting as either transition states or as unstable states which quickly revert back to the longer-lived

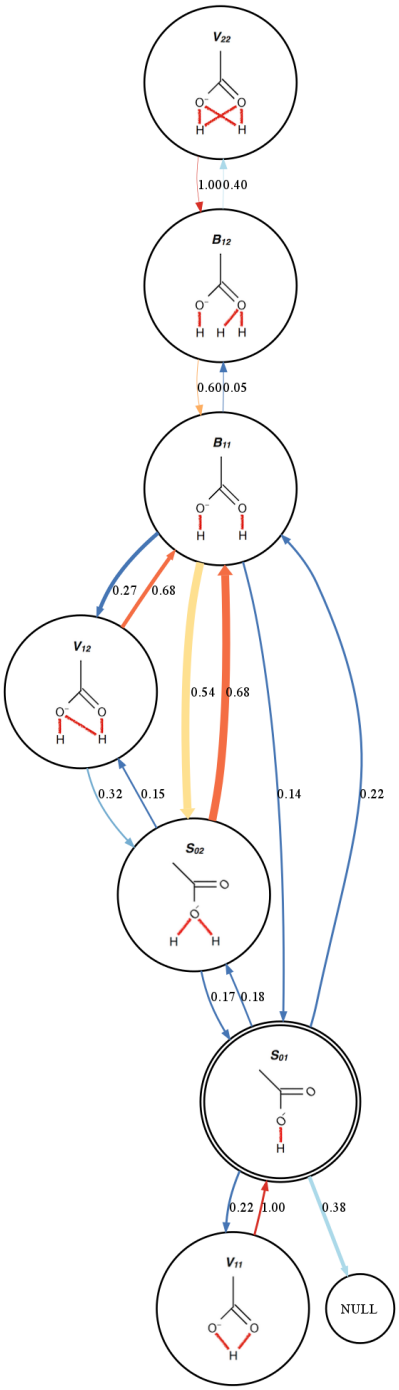

Fig. 5 H-bond transitions between different states for [C_2mim]Ac. Line width indicates the number of transitions between states. Color and arrow labels indicate the probability of the given path being taken.

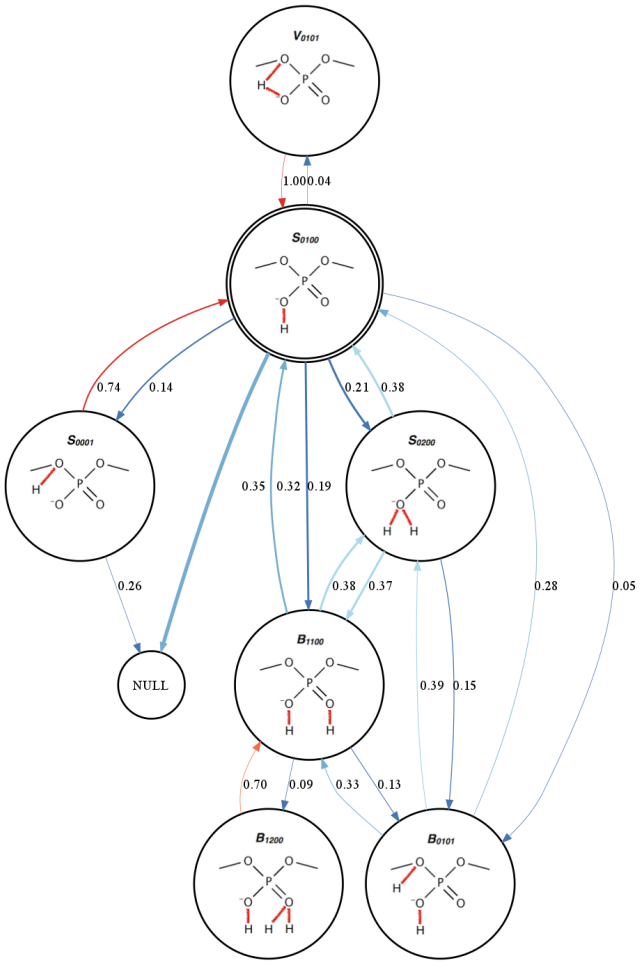

Fig. 6 H-bond transitions between different states for [C_2mim]DMP. Line width indicates the number of transitions between states. Color and arrow labels indicate the probability of the given path being taken.

state from which it was formed. The total time spent in a given state can be calculated by summing the lifetimes of all occurrences of a given state. If we look at the total fraction of the time spent in each of these states, we find that just two of these states account for roughly 95% of the total states observed and the three most populous states account for roughly 99% of observed states (see fig. 7). Regardless of the anion or the cation tail length the most populous state always seems to be S_1 which accounts for roughly 60% of the total states seen and corresponds to a single hydrogen bond formed with one of the anion's sites. Next is the S_2 state for chloride, the B_{11} state for acetate and the B_{1100} state for dimethylphosphate which each account for 30% of the states that are seen in their respective ILs. These three states are all very similar in that they are single anions bridging two different hydroxyl groups. If we consider that these three states are lower in energy than the singly bound $S_{01(00)}$ states, the main transitions toward the

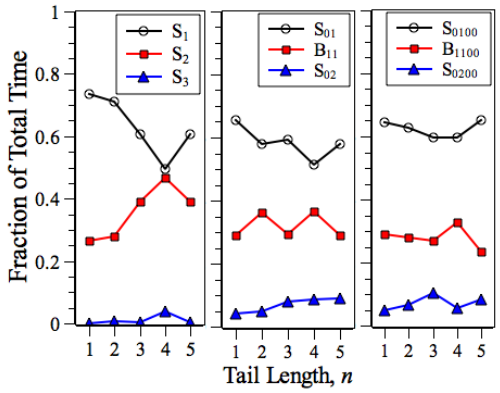

Fig. 7 Fraction of total time spent in the three most populous states as a function of the cation tail length. From left to right: chloride, acetate and dimethylphosphate.

promotion from the $S_{01(00)}$ state to the bridging states can occur either directly or via the $S_{02(00)}$ transition state (see fig. 8).

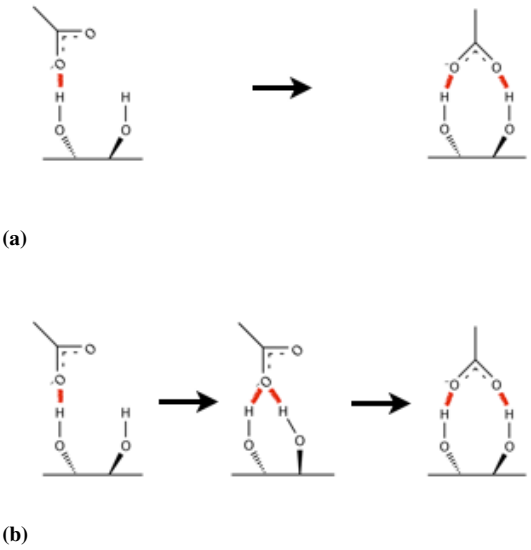

Fig. 8 Promotion of an acetate ion from the S_{01} state to the B_{11} state (a) directly and (b) via the S_{02} transition state.

Interestingly, the distance between the two hydrogen bond accepting oxygens in acetate and the POO^- oxygens in dimethylphosphate are very similar and are roughly the distance between successive hydroxyl groups within cellulose. As acetate and dimethylphosphate ions form single hydrogen bonds with cellulose, they lose a large proportion of their translational motion, yet retain their additional rotational degree of freedom, which is observed when comparing the mean squared displacement and mean squared angular displacements of the different anion states (see Supporting Information). The loss of translational motion ensures that the anion will remain in the vicinity of a neighboring hydroxyl group and through rotation and its "reach" be able to find it and form a hydrogen bond with it.

3.1.3 Bonding Lifetimes The arrows within fig. 4 show the average times of one state transitioning to another state. We are able to quantify the lifetimes of each individual state and determine, which states are more stable than others by looking at the average time that an anion remains in that one state before transitioning to any of the other possible states. These quantities are given in table 1. Here we are able to

Table 1 Mean lifetimes of different binding states, given in ps. States not listed in table all had lifetimes less than 20 ps.

Anion	State	Tail Length, n				
		1	2	3	4	5
Cl	S_1	331	325	248	191	263
	S_2	221	197	223	208	230
	S_3	26	70	30	103	31
Ac	S_{01}	406	350	278	266	323
	S_{02}	29	25	31	35	35
	B_{11}	173	151	107	118	92
	B_{12}	63	41	53	82	46
DMP	S_{0100}	169	153	130	153	147
	S_{0200}	27	29	31	28	33
	B_{1100}	148	120	94	132	100
	B_{1200}	23	36	36	25	39

clearly see that the lifetimes of the $S_{02(00)}$ states for all of the acetates and dimethylphosphates are roughly a third of the lifetimes of the B_{11} and B_{1100} states, respectively. These values are in agreement with our observation that for acetate and dimethylphosphate that S_{01} and S_{0100} were the most populous states, followed by B_{11} and B_{1100} and that S_{02} and S_{0200} were the third most populous state. This also supports our assertion in the previous section that the S_{02} state can be thought of as a kind of transition state between the $S_{01(00)}$ state to the bridging state $B_{11(00)}$.

Compared to the chloride anion, we note that the S_{02} and S_{0200} states for Ac and DMP are much shorter lived than the corresponding S_2 state for Cl. In examining the pathways connecting out of $S_{02(00)}$, however, the $B_{12(00)}$ state is never observed resulting directly from the $S_{02(00)}$ state, but can be accessed only from the $B_{11(00)}$ state. Given the relatively long transition times between the $B_{11(00)}$ state and its neighbors, with average lifetime of over 40 ps for Ac and 20 ps for DMP,

it is unlikely that such a transition occurred but was never observed in the simulations. This suggests that a doubly bonded oxygen must break at least one bond before the "paired" oxygen can successfully hydrogen bond.

Though the $S_{01(00)}$ state tends to be longer-lived than the B_{11} and B_{1100} states for both the acetates and the dimethylphosphates, this singly bound anion always remains just one hydrogen break away from becoming a free anion. Anions in the B_{11} and B_{1100} conversely, can endure the break of one of their two hydrogen bonds, reducing to the $S_{01(00)}$ state yet still remain a bound anion. This added redundancy in these bridging states not only adds to the hydrogen bonding energy of the anion, but it also ensures that the anion will remain bound with cellulose for a longer period of time. The average lifetime of acetate remaining bound with cellulose when beginning in different states is given in fig. 9.

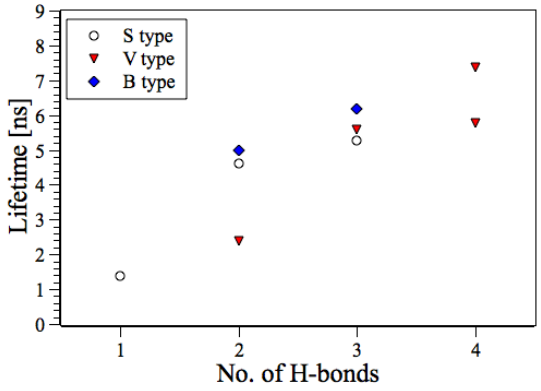

Fig. 9 Average lifetimes of acetate remaining bound with cellulose when beginning in various S-, B- and V-type states.

Anions in the B_{11} state (blue diamond with two hydrogen bonds) remain bound with cellulose over three times as long as anions in the S_{01} state (white circle with one H-bond). Furthermore anions in the V_{11} state (red triangle with two hydrogen bonds) have only slightly longer lifetimes than the S_{01} state while the S_{02} state (white circle with two hydrogen bonds) is also roughly three times as long as those in the S_{01} state. fig. 9 also clearly shows that the more hydrogen bonds that are formed with an anion, the longer it will remain bound with cellulose. More hydrogen bonds with a single anion add more layers of redundancy to the anion helping to ensure a longer lifetime of that anion remaining bound. An anion with four hydrogen bonds would have to undergo four hydrogen bond breaking events to become a free anion and in doing so would transition through a number of intermediate states, which could once again be promoted.

3.1.4 Individual Chains versus Bundles In addition to studying the interactions of the fifteen ILs with individual strands, we also performed simulations looking at the interactions with small bundles of cellulose Iβ consisting of ten strands with eight glucose units per strand. An overview of these results can be found in the Supporting Information. We find very few differences between the bundle simulations and the simulations with the individual strands. The most noticeable difference was the presence of higher-order binding patterns for each of the ILs, corresponding to more hydrogen bonds per anion. This was largely due to the mutual proximity of the neighboring strands, which effectively increases the local density of hydroxyl groups between the two strands. Therefore anions between the two strands have more hydroxyl groups available to them and have a higher probability of forming higher order binding patterns. These same higher-order binding patterns for the individual strands are only possible when different glucose units are brought into close proximity, either through strong kinks between neighboring units or looping of units from one end near the units of another ends, which tended to be very unlikely.

3.2 The Influence of Water Content

To better understand the influence of water on the hydrogen bonding behavior of the ionic liquids, additional simulations were performed for [C_2mim]Cl, [C_2mim]Ac and [C_2mim]DMP with 70 mol%, 80 mol% and 90 mol% water. The addition of water results in a significant reduction in the number of occurrences of every hydrogen bonding state. As the water content increases, the frequency of cellulose-IL hydrogen bonds continues to drop. A direct consequence of the reduction in each of the different states is a reduction in the average number of hydrogen bonds between the anions and cellulose that can be attributed to each state. Each of the three ILs showed a very similar reduction in the hydrogen bonding attributed to each state. Table 2 shows the trends in hydrogen bond formation for [C_2mim]Ac. Between 0 mol% and 70 mol%, the largest reduction in hydrogen bonding can be attributed to a steep reduction in the occurrence of the B_{11} state. At 70 mol% there are less than one-third as many hydrogen

Table 2 Average number of hydrogen bonds between acetate and cellulose in [C_2mim]Ac and associated with the four most populous states. Values are given on a per glucan basis.

State	0 mol%	70 mol%	80 mol%	90 mol%
S_{01}	1.05	0.91	0.73	0.49
B_{11}	0.73	0.22	0.20	0.08
S_{02}	0.15	0.31	0.23	0.11
B_{12}	0.03	0.04	0.04	0.01

bonds in the B_{11} state than bonds in the pure IL. Interestingly, while there is a steady reduction in the S_{01} hydrogen bonds as the water content increases, the frequency of the S_{02} state actually increases slightly.

The total number of hydrogen bonds per glucan for each of the three ILs as a function of the water content are given in table 3. At 90 mol% the total number of hydrogen bonds is

Table 3 Average number of hydrogen bonds per glucan unit for the three ILs as a function of the water concentration.

Water Conc.	$[C_2mim]Cl$	$[C_2mim]Ac$	$[C_2mim]DMP$
0 mol%	2.92	3.01	2.47
70 mol%	2.02	2.20	1.78
80 mol%	1.40	1.81	1.39
90 mol%	0.79	0.96	0.84

roughly one-third of the total for each of the corresponding pure ILs, showing that water significantly disrupts hydrogen bonding between the anion and cellulose. Compared with the other two ILs, $[C_2mim]Ac$ appears to be slightly less affected by the presence of water and maintains more hydrogen bonds with cellulose than the others for all four water concentrations. The transition pathways for the ILs with water were analyzed in a manner similar to that for the pure ILs, now taking into account the additional binding that involves water (see fig. 3). Beyond tracking the anion states that were bound in one way or another with cellulose, we also tracked the free anion states bound solely to water. It was found that the initial binding of an anion with cellulose occurred without water acting as a mediator. In other words, water bound to anions did not interact with cellulose and draw the two together. Instead, the binding of an anion with cellulose was first preceded by the unbinding of water from the anion and then the formation of a bond with cellulose in its place. For the acetate ion, fig. 10 depicts the mechanism behind the most frequent transitions between the S_{01}, S_{02} and B_{11} states.

Figure 10 shows the primary detachment mechanism from the B_{11} state through the S_{02} and S_{01} states to a free anion state. Each time a hydrogen bond between an anion and cellulose breaks, the open position on the anion is replaced by a new hydrogen bond with water. At the end, the free anion is bound by four waters, two on each oxygen. In this manner, water can be thought of as obstructing the hydrogen bonding sites of the anion, preventing them from interacting with cellulose. In reverse this shows the primary attachment mechanism and transition to the B_{11} state. Here, the water obstructing the hydrogen bond accepting sites of the anions must first detach before the anion can form a hydrogen bond with cellulose.

As shown shown earlier, the average number of hydrogen bonds in these higher-level states drops significantly as the water content increases. Another major consequence of increased water content in the ILs is an increase in the number of hydrogen bonds formed between the anions and water. This is true not only for the free anions but for anions that are bound with cellulose as well. This effect is shown for the free acetates of $[C_2mim]Ac$ in fig. 11. As the water content increases there is

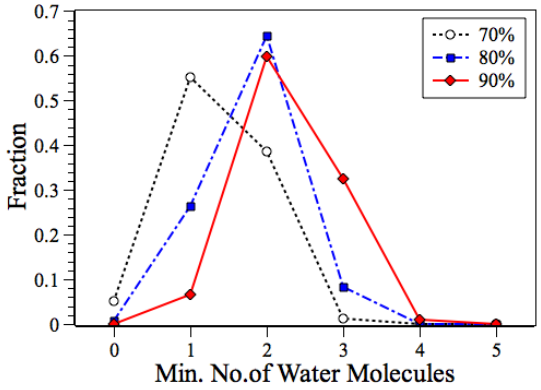

Fig. 11 Fraction of free acetates with a given minimal number of bound waters on either of the two oxygens.

a shift upward in the fraction of states with a given minimum number of waters bound to either of the two oxygens. For example, an acetate with two water molecules bound to one of the oxygens and just one water molecule bound to the other oxygen would have a minimum number of one, the lesser of the two values. Furthermore, a minimum value of zero is also possible, corresponding to a free acetate anion. For acetate it was found that the overwhelming majority of the transitions from the free state to the S_{01} state occurred when one of the acetate oxygens had just one bound water. If two or more waters were bound with each of the acetate oxygens, there was a dramatic decline in the number of transitions. Figure 11 shows that as the water content increases from 70 to 90 mol%, the fraction of acetates with just one bound water on either of the oxygens drops from 0.55 to 0.25 and finally to 0.05. Thus at higher water concentrations there are significantly fewer free anions in the bulk with sufficiently unobstructed hydrogen bonding sites that can interact with cellulose. Similarly, when an anion is in a higher level state such as B_{11} and a hydrogen bond breaks, there is a much higher probability that the site will be replaced with the readily available water molecules, significantly reducing the chances that the hydrogen bond with cellulose will reform.

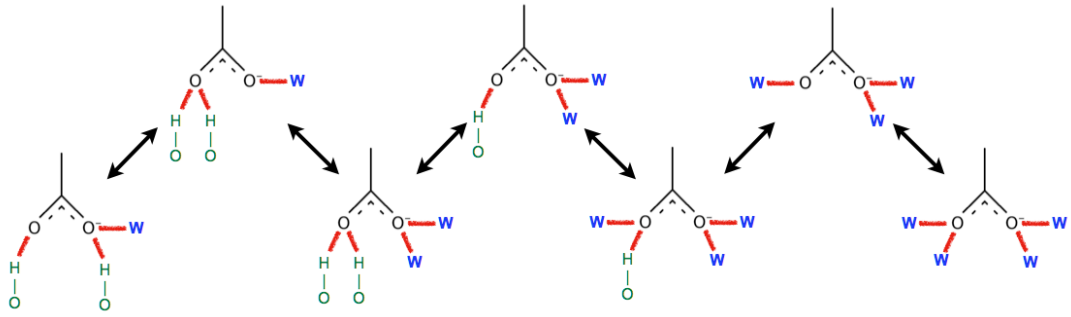

Fig. 10 Typical path of a free acetate anion to and from the B_{11} state when water is present.

4 Conclusions

We have mapped the transitions in the hydrogen bonding states of anions bound to cellulose. We observed a complex series of transitions for each of the anions, although, for each IL, just three states account for roughly 95% of all of the observed states. We found that singly bound anions (S_1) account for roughly 60% of the states, while another 30% of the observed states were "bridging" states composed of two hydrogen bonds, one at each of the two hydrogen bond accepting sites within the anion. Once a Ac or DMP anion is hydrogen bonded to a hydroxyl group within cellulose, it has the rotational freedom and reach to find a neighboring hydroxyl group within cellulose and form a second hydrogen bond with its second acceptor site, effectively becoming a bridging state. Furthermore, a short-lived intermediate state composed of two hydroxyl groups within cellulose both hydrogen bonded to only one of the two oxygens within the Ac or DMP anion can help guide the promotion of the singly bound state to the stable bridging state. The transition of an anion from the singly bound state to the bridging state, and the ensuing hydrogen bonding redundancy, increases the lifetime of the anion remaining bound with cellulose by roughly 3 to 4 times that of the singly bound state. The replacement of the dense hydrogen bonding network with crystalline cellulose with strong, plentiful and long-lived hydrogen bonds with the IL solvent is at the heart of the dissolution process. We find that anions having these multiple hydrogen bond acceptors with optimal spacing can significantly increase the hydrogen bonding interaction between ionic liquids and cellulose this helping to promote dissolution.

In the presence of water, the formation of the bridging states are disproportionately affected, leading to large drops in the overall numbers of hydrogen bonds formed between the anions and cellulose. We find that water forms hydrogen bonds with the acceptor sites of the anions, obstructing further interactions with cellulose. Moreover, when a hydrogen bond between the anion and cellulose breaks, the free site is quickly replaced preventing further contact with cellulose. For a new hydrogen bond to form between the anion and cellulose, an obstructing water must first detach from the anion and make way for the new bond. As the water concentration increases, this process occurs significantly less often, preventing anions from interacting with cellulose and thus reducing the number of anion–cellulose hydrogen bonds.

5 Acknowledgments

This work was performed as part of the Cluster of Excellence "Tailor-Made Fuels from Biomass," which is funded by the Excellence Initiative by the German federal and state governments to promote science and research at German universities.

References

1 R. Atalla and D. Vanderhart, *Science*, 1984.
2 C. M. Altaner, L. H. Thomas, A. N. Fernandes and M. C. Jarvis, *Biomacromolecules*, 2014.
3 Y. Nishiyama, P. Langan and H. Chanzy, *J Am Chem Soc*, 2002, **124**, 9074–9082.
4 A. S. Gross and J.-W. Chu, *J Phys Chem B*, 2010, **114**, 13333–13341.
5 G. T. Beckham, J. F. Matthews, B. Peters, Y. J. Bomble, M. E. Himmel and M. F. Crowley, *J Phys Chem B*, 2011, **115**, 4118–4127.
6 C. M. Payne, M. E. Himmel, M. F. Crowley and G. T. Beckham, *J Phys Chem Lett*, 2011, **2**, 1546–1550.
7 P. N. Ciesielski, J. F. Matthews, M. P. Tucker, G. T. Beckham, M. F. Crowley, M. E. Himmel and B. S. Donohoe, *ACS Nano*, 2013.
8 J. Viell and W. Marquardt, *Holzforschung*, 2011, **65**, 519–525.
9 G. Cheng, P. Varanasi, R. Arora, V. Stavila, B. A. Simmons, M. S. Kent and S. Singh, *J Phys Chem B*, 2012, **116**, 10049–54.
10 H. Liu, G. Cheng, M. Kent, V. Stavila, B. A. Simmons, K. L. Sale and S. Singh, *J Phys Chem B*, 2012.
11 Z. Jarin and J. Pfaendtner, *J Chem Theory Comput*, 2014, **10**, 507–510.
12 B. Mostofian, X. Cheng and J. Smith, *The Journal of Physical . . .* , 2014.
13 G. Cheng, P. Varanasi, C. Li, H. Liu, Y. B. Menichenko, B. A. Simmons, M. S. Kent and S. Singh, *Biomacromolecules*, 2011, **12**, 933–941.
14 A. A. Niazi, B. D. Rabideau and A. E. Ismail, *J Phys Chem B*, 2013, **117**, 1378–88.
15 Y. Chen, Y. Cao, X. Sun and T. Mu, *Journal of Molecular Liquids*, 2014, **190**, 151 – 158.

16 H. Liu, K. L. Sale, B. A. Simmons and S. Singh, *J Phys Chem B*, 2011, **115**, 10251–10258.
17 K. Gupta, Z. Hu and J. Jiang, *RSC Advances*, 2013.
18 Y. Zhao, X. Liu, J. Wang and S. Zhang, *The journal of physical chemistry B*, 2013, **117**, 9042–9049.
19 F. Huo, Z. Liu and W. Wang, *J Phys Chem B*, 2013.
20 S. Bylin, C. Olsson, G. Westman and H. Thielander, *Bioresources*, 2013, **9**, 1038–1054.
21 R. Rinaldi, *Chem Commun*, 2011, **47**, 511–513.
22 A. Pinkert, K. N. Marsh and S. Pang, *Ind Eng Chem Res*, 2010, **49**, 11121–11130.
23 H. Wang, G. Gurau and R. D. Rogers, *Chem Soc Rev*, 2012, **41**, 1519–1537.
24 A. Brandt, J. Grasvik, J. P. Hallett and T. Welton, *Green Chemistry*, 2013, **15**, 550–583.
25 A. M. da Costa Lopes, K. G. João and A. Morais, *Sustain Chem . . .*, 2013.
26 K. M. Gupta, Z. Hu and J. Jiang, *Polymer*, 2011, **52**, 5904–5911.
27 R. C. Remsing, R. P. Swatloski, R. D. Rogers and G. Moyna, *Chem Commun*, 2006, 1271.
28 M. Zavrel, D. Bross, M. Funke, J. Buechs and A. C. Spiess, *Bioresource Technol*, 2009, **100**, 2580–2587.
29 Y. Fukaya, K. Hayashi, M. Wada and H. Ohno, *Green Chem*, 2008, **10**, 44–46.
30 L. Crowhurst and P. Mawdsley. . . , *Phys Chem Chem Phys*, 2003, **5**, 2790–2794.
31 A. Brandt, J. Hallett, D. Leak, R. Murphy and T. Welton, *Green Chem*, 2010.
32 *Cellulose Solvents: For Analysis, Shaping and Chemical Modification*, OUP USA, 2010.
33 R. S. Payal and S. Balasubramanian, *Physical Chemistry Chemical Physics*, 2014, **16**, 17458–17465.
34 R. S. Payal, R. Bharath, G. Periyasamy and S. Balasubramanian, *J Phys Chem B*, 2012, **116**, 833–840.
35 J. Zhang, H. Zhang, J. Wu, J. Zhang, J. He and J. Xiang, *Phys Chem Chem Phys*, 2010, **12**, 1941.
36 H. Liu, K. L. Sale, B. M. Holmes, B. A. Simmons and S. Singh, *J Phys Chem B*, 2010, **114**, 4293–4301.
37 T. G. A. Youngs, C. Hardacre and J. D. Holbrey, *J Phys Chem B*, 2007, **111**, 13765–13774.
38 T. G. A. Youngs, J. D. Holbrey, C. L. Mullan, S. E. Norman, M. C. Lagunas, C. D'Agostino, M. D. Mantle, L. F. Gladden, D. T. Bowron and C. Hardacre, *Chem Sci*, 2011, **2**, 1594–1605.
39 B. D. Rabideau and A. E. Ismail, *J Phys Chem B*, 2012, **116**, 9732–43.
40 B. D. Rabideau, A. Agarwal and A. E. Ismail, *J Phys Chem B*, 2013, **117**, 3469–3479.
41 B. Lindman, G. Karlström and L. Stigsson, *J Molec Liq*, 2010.
42 H. M. Cho, A. S. Gross and J.-W. Chu, *J Am Chem Soc*, 2011, **133**, 14033–14041.
43 A. S. Gross, A. T. Bell and J.-W. Chu, *J Phys Chem B*, 2011, **115**, 13433–13440.
44 B. D. Rabideau, A. Agarwal and A. E. Ismail, *J Phys Chem B*, 2014, **118**, 1621–1629.
45 T. G. A. Youngs, J. D. Holbrey, M. Deetlefs, M. Nieuwenhuyzen, M. F. C. Gomes and C. Hardacre, *ChemPhysChem*, 2006, **7**, 2279–2281.
46 S. Plimpton, *J Comput Phys*, 1995, **117**, 1–19.
47 J. N. Canongia Lopes, J. Deschamps and A. A. H. Padua, *J Phys Chem B*, 2004, **108**, 2038–2047.
48 J. N. Canongia Lopes, J. Deschamps and A. A. H. Padua, *J Phys Chem B*, 2004, **108**, 11250–11250.
49 W. Jorgensen, D. Maxwell and J. Tirado-Rives, *J Am Chem Soc*, 1996, **118**, 11225–11236.
50 W. Jorgensen, J. Chandrasekhar, J. Madura, R. Impey and M. Klein, *J Chem Phys*, 1983, **79**, 926–935.
51 J. Ryckaert, G. Ciccotti and H. Berendsen, *J Comput Phys*, 1977, **23**, 327–341.
52 R. W. Hockney and J. W. Eastwood, *Computer Simulation Using Particles*, Adam Hilger-IOP, Bristol, U. K., 1988.
53 S. Chowdhuri and A. Chandra, *Phys Rev E*, 2002, **66**, 041203.
54 A. Chandra, *Phys Rev Lett*, 2000, **85**, 768–771.
55 A. Luzar and D. Chandler, *Phys Rev Lett*, 1996, **76**, 928–931.
56 A. Luzar, *J Chem Phys*, 2000, **113**, 10663–10675.
57 A. Luzar and D. Chandler, *J Chem Phys*, 1993, **98**, 8160–8173.
58 A. Luzar and D. Chandler, *Nature*, 1996, **379**, 55–57.
59 I. Skarmoutsos, D. Dellis, R. P. Matthews, T. Welton and P. A. Hunt, *The journal of physical chemistry B*, 2012, **116**, 4921–4933.
60 I. Skarmoutsos, T. Welton and P. A. Hunt, *Physical Chemistry Chemical Physics*, 2014, **16**, 3675–3685.